Effect of different carboxylic acids on the aromatic hydroxylation with H$_2$O$_2$ in the presence of an iron aminopyridine complex

Nikolay V. Tkachenko [a, b], Oleg Y. Lyakin [a, b], Alexandra M. Zima [a, b], Evgenii P. Talsi [a, b], Konstantin P. Bryliakov [a, b, *]

[a] Boreskov Institute of Catalysis, Pr. Lavrentieva 5, Novosibirsk, 630090, Russia
[b] Novosibirsk State University, Pirogova 2, Novosibirsk, 630090, Russia

ARTICLE INFO

ABSTRACT

In this contribution, the effect of the structure of the catalytic additive − carboxylic acid − on the catalytic performance of the iron based catalyst [(PDP)Fe(OTf)$_2$], **2** (PDP = N,N′-bis(2-pyridylmethyl)-(S,S)-2,2′-bipyrrolidine) in the selective aromatic oxidation of alkylbenzenes with H$_2$O$_2$ is presented. Eight (linear and branched) carboxylic acids have been tested; in the presence of 2-ethylhexanoic acid, the system [(PDP)Fe(OTf)$_2$]/RCOOH/H$_2$O$_2$ has demonstrated the highest substrate conversion and the highest selectivity for oxygen incorporation into the aromatic ring (up to > 99%) at the same time. Low-temperature EPR spectroscopic study of the system [(PDP)Fe(OTf)$_2$]/2-ethylhexanoic acid/H$_2$O$_2$ witness the presence of the low-spin perferryl intermediate **2a^{EHA}** with small g-factor anisotropy ($g_1 = 2.069$, $g_2 = 2.007$, $g_3 = 1.963$), which directly reacts with benzene at $-80\,°C$ with the rate constant $k_2 = 0.6\,M^{-1}s^{-1}$, and with toluene with $k_2 > 1\,M^{-1}s^{-1}$, thus giving evidence for its key role in the selective oxygenation of aromatic substrates.

© 2018 Elsevier B.V. All rights reserved.

1. Introduction

Chiral bipyrrolidine-derived iron complexes of the PDP family (PDP = N,N′-bis(2-pyridylmethyl)-2,2′-bipyrrolidine) have emerged as very fruitful, active and efficient biomimetic catalysts for the oxidation of olefinic C=C and aliphatic C—H groups with hydrogen peroxide [1—9], as well as for the aerobic asymmetric oxidative C—C coupling of 2-naphthols [10]. At the same time, in aromatic hydroxylation reactions [11—18], Fe(PDP) complexes have not been represented until very recently [19,20].

Encouragingly, in 2018 we have found that iron complex [(PDP*)Fe^{III}(μ-OH)$_2$Fe^{III}(PDP*)](OTf)$_4$, **1** (PDP* = N,N′-bis(3,5-dimethyl-4-methoxypyridyl-2-methyl)-(S,S)-2,2′-bipyrrolidine, Fig. 1) is capable of mediating the hydroxylation of aromatic substrates (benzene and substituted benzenes) with H$_2$O$_2$, with good efficiency (up to 36.5 TN) and high selectivity for oxygen incorporation into the aromatic ring (up to 91%) [19]. Subsequently, a series of iron-PDP complexes, bearing different substituents at the PDP ligands, and different counteranions, have been tested in the

oxidation of alkylaromatic compounds with H$_2$O$_2$, and the parent complex [(PDP)Fe(OTf)$_2$] (**2**) has been identified as the most efficient catalyst, performing up to 84 catalytic turnovers under the reaction conditions and demonstrating higher aromatic oxygenation selectivity (up to 93%) [20].

So far, acetic acid (AA) has been used as the additive in Fe(PDP)-catalyzed aromatic hydroxylations with H$_2$O$_2$ [19,20]. In this work, we present a systematic study of different (linear and branched) carboxylic acids in these reactions, catalyzed by complex **2**, witnessing that 2-ethylhexanoic (EHA) acid has optimal structure, ensuring the highest conversion and aromatic oxidation selectivity. Noticeably, according to the EPR data, the high-valent iron species observed in the presence of AA and EHA are different: the low-spin complex with large g-factor anisotropy **2a^{AA}** ($g_1 = 2.66$, $g_2 = 2.42$, $g_3 = 1.71$) and the low-spin complex with small g-factor anisotropy **2a^{EHA}** ($g_1 = 2.069$, $g_2 = 2.007$, $g_3 = 1.963$). The results of evaluation of their reactivity toward arenes at low temperature are reported.
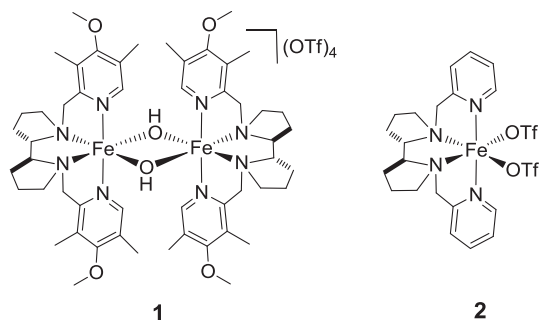
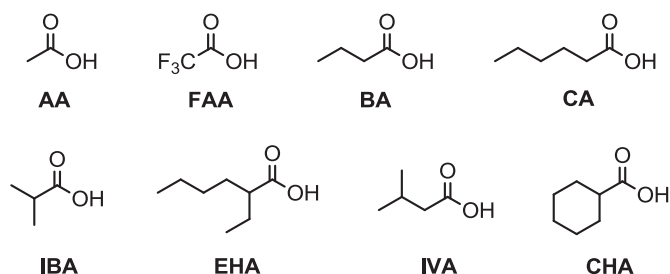Fig. 1. Structures of complexes 1 and 2 discussed in this work.

Fig. 2. Structures and abbreviations of carboxylic acids used in this work.
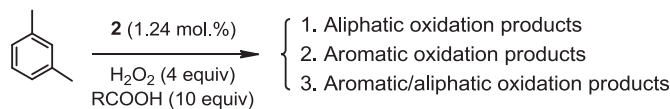
2. Experimental section

Iron complexes **1** and **2** were prepared as described [21,22]. Catalytic oxidations were conducted as follows: aromatic substrate (0.10 mmol), followed by carboxylic acid (10 equiv., 1.0 mmol), was added to the solution of iron complex **2** (1.24 μmol) in CH$_3$CN (0.40 mL), and the solution was thermostated at 0 °C. The solution of H$_2$O$_2$ (4 equiv., 0.40 mmol) in CH$_3$CN (total volume 0.10 mL) was injected to the reaction mixture by a syringe pump over 30 min upon stirring. The reaction mixture was stirred for 2.5 h at 0 °C and then analyzed by GC/MS.

Detailed experimental data can be found in the Supplementary data.
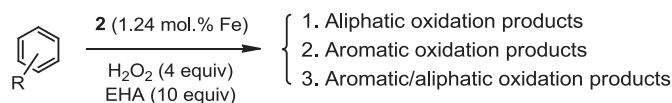
3. Results and discussion

3.1. Effect of the structure of carboxylic acid on the catalytic performance of complex **2**

First of all, different carboxylic acids (Fig. 2) were tested as additives in the oxidation of *m*-xylene by the catalyst systems **2**/RCOOH/H$_2$O$_2$ under the same optimized conditions [19,20]. The results are collected in Table 1. For alkylbenzenes, the reaction mixtures contained the products of aromatic oxidation (containing oxygen at the aromatic ring), aliphatic oxidation (containing oxygen at alkyl side chain) and aromatic/aliphatic oxidation (containing oxygen both at the aromatic ring and at alkyl side chain). In agreement with the previously used approach [19,20], the aromatic oxidation selectivity was calculated as {amount of aromatic oxidation products + amount of aromatic/aliphatic oxidation products}/overall amount of oxidation products. Minor unidentified products, if any, were not taken into calculation, owing to the impossibility of their identification and reliable quantification. The mass balance was typically better than 95%.

With trifluoroacetic acid, the yield of oxidized products dropped substantially (Table 1, entry 1). As a general trend, the use of branched acids (entries 6–8) led to higher yields of oxidized products, compared with linear acids (entries 2–4); at the same time, the selectivity for aromatic oxidation was higher with branched acids, in some cases exceeding 99% (entries 2–8). Gratifyingly, 2-ethylhexanoic acid, previously established as probably one of the most effective additives in Fe and Mn catalyzed asymmetric epoxidation reactions [5–7,9,23–26], ensured the highest yield of oxygenated products and the highest aromatic oxidation selectivity at the same time (entry 8). Without added carboxylic acid, inferior substrate conversion and aromatic oxidation selectivity was obtained (entry 9 of Table 1).

Next, the oxidation of different substrates by system **2**/EHA/H$_2$O$_2$ was studied (Table 2). In most cases, the aromatic oxidation selectivity was higher than 95% (entries 2, 3, 5–9). For several substrates, aromatic oxidation selectivity of up to 99% was achieved (entries 2, 5, 6, 7). Interestingly, the oxidation of *m*-xylene occurred with preferential formation of 2,6-dimethylhydroquinone (entry 7 of Table 2; entry 7 of Table S2). For all substrates, system **2**/EHA/H$_2$O$_2$ demonstrated higher aromatic oxidation selectivities than

Table 1
Catalytic oxidation of *m*-xylene with H$_2$O$_2$ in the presence of complexes **2**.[a]

Entry	Carboxylic acid	Conversion (%)	Aliphatic oxidation[b]	Aromatic oxidation[b]	Aromatic/aliphatic[b]	Selectivity for aromatic oxidation (%)[c]	TN[d]
1	FAA	1.6	0.5	0.6	0.2	62	1.9
2	AA	67.0	0.8	32.0	17.4	98	96.8
3	CA	17.5	0.6	6.2	6.8	96	25.6
4	BA	46.4	0.4	20.5	14.3	99	67.4
5	CHA	31	0.2	13.4	9.1	99	40.3
6	IBA	75.1	0.3	31.7	24.3	99	109.9
7	IVA	83.3	–	26.8	35.1	>99	120.8
8	EHA	98.3	–	51.6	26.2	>99	151.9
9	–[e]	8.0	4.3	3.1	2.2	55	17.5

[a] Conditions: 0 °C; *m*-xylene (0.10 mmol), H$_2$O$_2$ (0.40 mmol), RCOOH (1.0 mmol), catalyst (1.24 μmol), CH$_3$CN (0.40 mL), syringe-pump addition of H$_2$O$_2$ during 30 min, followed by 2.5 h stirring.

[b] Yields, moles of products/mole of Fe. Detailed compositions of the reaction mixtures are provided in Table S1, Supplementary data.

[c] Calculated as 100%·{"aromatic oxidation products" + "aromatic/aliphatic oxidation products"}/overall amount of identified oxidation products.

[d] TN defined as {moles of single oxidation products/mole of Fe}+2{moles of double oxidation products/mole of Fe}. Ketones and aldehydes were considered as double oxidation products.

[e] Carboxylic acid was not added; 3 mmol of exogenous H$_2$O was present in the reaction mixture from the beginning of the reaction.

Table 2
Catalytic oxidation of aromatic substrates with H_2O_2 in the presence of complex **2**.[a]

2 (1.24 mol.% Fe)

H_2O_2 (4 equiv)
EHA (10 equiv)

1. Aliphatic oxidation products
2. Aromatic oxidation products
3. Aromatic/aliphatic oxidation products

Entry	Substrate	Conversion (%)	Aliphatic oxidation[b]	Aromatic oxidation[b]	Aromatic/aliphatic[b]	Selectivity for aromatic oxidation (%)[c]	TN[d]
1	benzene	13.8	–	11.1	–	–	22.0
2	toluene	28.8	0.3	18.2	4.7	99	43.9
3	ethylbenzene	19.5	0.8	11.1	3.8	95	29.6
4	cumene	13.9	0.6	9.2	1.1	94	19.7
5	isobutylbenzene	19.7	0.1	12.1	3.3	99	29.7
6	o-xylene	35.8	0.1	20.4	8.4	99	56.3
7	m-xylene	98.3	–	51.6	26.2	>99	151.9
8	p-xylene	43.5	0.6	27.1	6.4	98	65.3
9	2-ethyltoluene	34.0	0.4	15.2	7.3	98	44.5
10	3-ethyltoluene	24.8	1.3	14.6	3.8	93	36.4
11	4-ethyltoluene	45.5	2.5	30.3	2.6	93	67.7

[a] Conditions: 0 °C; substrate (0.10 mmol), H_2O_2 (0.40 mmol), EHA (1.0 mmol), catalyst (1.24 μmol), CH_3CN (0.40 mL), syringe-pump addition of H_2O_2 during 30 min, followed by 2.5 h stirring.
[b] Yields, moles of products/mole of Fe. Detailed compositions of the reaction mixtures are provided in Table S2, Supplementary data.
[c] Calculated as 100%·{"aromatic oxidation products" + "aromatic/aliphatic oxidation products"}/overall amount of identified oxidation products.
[d] TN defined as {moles of single oxidation products/mole of Fe}+2{moles of double oxidation products/mole of Fe}. Ketones and aldehydes were considered as double oxidation products.

system **2**/AcOH/H_2O_2 [20]; the substrate conversions demonstrated by the **2**/EHA/H_2O_2 system were either higher or similar to those by the **2**/AcOH/H_2O_2 system.

3.2. EPR spectroscopic study of the iron-oxo intermediates

In order to get the insight into the reason of the high aromatic oxidation selectivity of the catalyst system **2**/EHA/H_2O_2, formation of the high-valent iron intermediates in this system was monitored by EPR spectroscopy at low temperature.

Previously, we showed that the catalyst systems **2**/AA/H_2O_2 and **2**/EHA/H_2O_2, display highly unstable intermediates **2a^{AA}** and **2a^{EHA}** (Table 3) with strictly different EPR spectra $g_1 = 2.66$, $g_2 = 2.42$, $g_3 = 1.71$ and $g_1 = 2.069$, $g_2 = 2.007$, $g_3 = 1.963$, respectively [7]. These intermediates are highly unstable and can be generated and monitored only at temperatures as low as −80 … −70 °C. The intermediate **2a^{EHA}** was assigned to the oxoiron(V) species on the basis of the close similarity of its EPR spectrum to that of well spectroscopically characterized oxoiron(V) species [7,27,28], whereas the structure of intermediate **2a^{AA}** remains debatable [29].

The catalyst systems **1**/AA/H_2O_2 and **1**/EHA/H_2O_2, exhibit intermediates **1a^{AA}** and **1a^{EHA}** at −80 … −70 °C with virtually identical EPR spectra ($g_1 = 2.07$, $g_2 = 2.007$, $g_3 = 1.96$), nearly coinciding with that of **2a^{EHA}** (Table 3). The same intermediates are formed in the catalyst systems **1**/AA/CH_3CO_3H and **1**/EHA/CH_3CO_3H [9,19]. However, in the systems with CH_3CO_3H their maximum concentration is several times higher than in the systems with H_2O_2. Very recently, the direct reactivity of intermediates **1a^{AA}** and **1a^{EHA}** (formed in the catalyst systems **1**/RCOOH/CH_3CO_3H) toward

cyclohexane and substituted benzenes was evaluated [19,30].

Herein, we have evaluated the reactivity of intermediate **2a^{EHA}**, generated in the catalyst system **2**/EHA/H_2O_2, toward benzene at −80 °C. As was shown previously, the catalyst systems **1**/AA/CH_3CO_3H and **1**/EHA/CH_3CO_3H display maximum concentration of **1a^{AA}** and **1a^{EHA}** just after mixing the reagents at −70 °C, and then their concentration decreases [19]. In contrast, the concentration of **2a^{EHA}** formed in system **2**/EHA/H_2O_2 is quasi-stationary during 5−10 min after the reaction onset at −80 °C, and then decreases (Fig. 3A). The first order rate constant $k_1 = (4 \pm 1) \times 10^{-3}$ s^{-1} of the intermediate **2a^{EHA}** self-decay can be determined from the decrease of its concentration with time after the quasi-stationary period (Fig. 3C). In the presence of benzene (0.04 M), the quasi-stationary concentration of **2a^{EHA}** was 7 times lower (Fig. 3B and C). These data allowed the evaluation of the second-order rate constant k_2 for the reaction of **2a^{EHA}** with benzene at −80 °C from the equation $(k_1 + k_2 \cdot [C_6H_6])/k_1 = 7$. The resulting $k_2 = 0.6 \pm 0.2$ M^{-1}s^{-1} is at least one order of magnitude lower than the corresponding value of $k_2 > 10$ M^{-1}s^{-1}, evaluated for the reaction of **1a^{EHA}** with benzene at −70 °C [19].

More electron-rich substrate, toluene, reacted with **2a^{EHA}** more readily, so that in the presence of toluene (0.04), the concentration of **2a^{EHA}** was below the detection limit. This indicates that the corresponding value of k_2 is noticeably larger than 1 M^{-1}s^{-1}.

Intriguingly, the self-decay of the intermediate **2a^{AA}** with large g-factor anisotropy in system **2**/AA/H_2O_2 did not accelerate in the presence of either benzene (0.04 M) at −80 °C or more electron-rich pseudocumene (0.04 M). This apparent contradiction to the observation of direct reactivity of the intermediates with large g-factor anisotropy in closely structurally related catalyst systems toward organic substrates [31,32] is at the moment not well understood and requires further studies. Presumably, the different reactivities of the key iron-oxygen species, **2a^{EHA}** and **2a^{AA}** may be connected with the different aromatic oxidation selectivities of the corresponding catalyst systems **2**/EHA/H_2O_2 and **2**/AA/H_2O_2.

4. Conclusions

Iron complex [(PDP)Fe(OTf)$_2$] (**2**) efficiently catalyzes the aromatic hydroxylation of alkylarenes (substituted benzenes) with

Table 3
EPR spectroscopic data (CH_3CN/CH_2Cl_2, 77 K) for $S = 1/2$ aminopyridine iron-oxo intermediates observed in the catalyst systems **1**/RCOOH/H_2O_2 and **2**/RCOOH/H_2O_2 (RCOOH = AA or EHA).

No	Intermediate	g_1	g_2	g_3	ref.
1	[(PDP*)Fe^V=O(OC(O)R)]$^{2+}$ (**1a^{EHA}**)	2.070	2.008	1.958	7
2	[(PDP*)Fe^V=O(OC(O)CH$_3$)]$^{2+}$ (**1a^{AA}**)	2.071	2.008	1.960	21
3	[(PDP)Fe^V=O(OC(O)R)]$^{2+}$ (**2a^{EHA}**)	2.069	2.007	1.963	7
4	**2a^{AA}**	2.66	2.42	1.71	5, 7

Fig. 3. (A) EPR spectra (−196 °C) of the sample **2**/H₂O₂/EHA ([Fe]:[H₂O₂]:[EHA] = 1:3:10, [Fe] = 0.04 M), frozen after mixing the reagents during 2 min at −70 °C in a CH₂Cl₂/CH₃CN mixture (v/v = 1.8:1) and storing the sample at −80 °C for various times seen from the dark-blue point set in "C". (B) EPR spectra (−196 °C) of the sample in "A" with the addition of benzene (0.04 M) just after recording the first spectrum (storage time at −80 °C is seen from the brown point set in "C"). (C) Concentration of **2a^{EHA}** vs. sample storage time at −80 °C calculated from the intensities of its EPR resonance at $g_2 = 2.007$ in "A" (dark-blue) and "B" (brown). Asterisks denote the EPR signal of an unknown iron complex formed upon the decay of **2a^{EHA}**. (For interpretation of the references to colour in this figure legend, the reader is referred to the Web version of this article.)

hydrogen peroxide in the presence of different carboxylic acids, performing up to 157 catalytic turnovers. 2-Ethylhexanoic acid ensures the highest selectivity of the catalyst system for oxygen incorporation into the aromatic ring (up to 99%) and the highest yield of oxygenated products at the same time. EPR spectroscopic study of the low-spin active species **2a^{EHA}** with small g-factor anisotropy ($g_1 = 2.069$, $g_2 = 2.007$, $g_3 = 1.963$) in the system [(PDP) Fe(OTf)₂]/EHA/H₂O₂ allows evaluating the apparent rate constant for the direct reaction of **2a^{EHA}** with benzene ($k_2 = 0.6 \pm 0.2\,M^{-1}s^{-1}$) and toluene ($k_2 > 1\,M^{-1}s^{-1}$) at −80 °C, thus supporting the key role of **2a^{EHA}** in the selective oxygenation of aromatic substrates. Further

studies, aimed at disclosing the nature of the iron intermediates with large g-factor anisotropy, are underway.

Appendix A. Supplementary data

Supplementary data related to this article can be found at https://doi.org/10.1016/j.jorganchem.2018.07.016.

References

[1] M.S. Chen, M.C. White, A predictably selective aliphatic C−H oxidation reaction for complex molecule synthesis, Science 318 (2007) 783−787.
[2] M.S. Chen, M.C. White, Combined effects on selectivity in Fe-catalyzed methylene oxidation, Science 327 (2010) 566−571.
[3] M.A. Bigi, S.A. Reed, M.C. White, Diverting non-haem iron catalysed aliphatic C−H hydroxylations towards desaturations, Nat. Chem. 3 (2011) 216−222.
[4] M.A. Bigi, S.A. Reed, M.C. White, Directed metal(oxo) aliphatic C−H hydroxylations: overriding substrate bias, J. Am. Chem. Soc. 134 (2012) 9721−9726.
[5] O.Y. Lyakin, R.V. Ottenbacher, K.P. Bryliakov, E.P. Talsi, Asymmetric epoxidations with H₂O₂ on Fe and Mn aminopyridine catalysts: probing the nature of active species by combined electron paramagnetic resonance and enantioselectivity study, ACS Catal. 2 (2012) 1196−1202.
[6] O. Cussó, I. Garcia-Bosch, X. Ribas, J. Lloret-Fillol, M. Costas, Asymmetric epoxidation with H₂O₂ by manipulating the electronic properties of non-heme iron catalysts, J. Am. Chem. Soc. 135 (2013) 14871−14878.
[7] A.M. Zima, O.Y. Lyakin, R.V. Ottenbacher, K.P. Bryliakov, E.P. Talsi, Dramatic effect of carboxylic acid on the electronic structure of the active species in Fe(PDP)-catalyzed asymmetric epoxidation, ACS Catal. 6 (2016) 5399−5404.
[8] D. Font, M. Canta, M. Milan, O. Cussó, X. Ribas, R.J.M. Klein Gebbink, M. Costas, Readily accessible bulky iron catalysts exhibiting site selectivity in the oxidation of steroidal substrates, Angew. Chem. Int. Ed. 55 (2016) 5776−5779.
[9] A.M. Zima, O.Y. Lyakin, R.V. Ottenbacher, K.P. Bryliakov, E.P. Talsi, Iron-catalyzed enantioselective epoxidations with various oxidants: evidence for different active species and epoxidation mechanisms, ACS Catal. 7 (2017) 60−69.
[10] N.V. Tkachenko, O.Y. Lyakin, D.G. Samsonenko, E.P. Talsi, K.P. Bryliakov, Highly efficient asymmetric aerobic oxidative coupling of 2-naphthols in the presence of bioinspired iron aminopyridine complexes, Catal. Commun. 104 (2018) 112−117.
[11] S. Taktak, M. Flook, B.M. Foxman, L. Que Jr., E.V. Rybak-Akimova, ortho-Hydroxylation of benzoic acids with hydrogen peroxide at a non-heme iron center, Chem. Commun. (2005) 5301−5303.
[12] A. Thibon, J.-F. Bartoli, R. Guillot, J. Sainton, M. Martinho, D. Mansuy, F. Banse, Non-heme iron polyazadentate complexes as catalysts for aromatic hydroxylation by H₂O₂: particular efficiency of tetrakis(2-pyridylmethyl)ethylenediamine−iron(II) complexes, J. Mol. Catal. A: Chem. 287 (2008) 115−120.
[13] O.V. Makhlynets, E.V. Rybak-Akimova, Aromatic hydroxylation at a non-heme iron center: observed intermediates and insights into the nature of the active species, Chem. Eur. J. 16 (2010) 13995−14006.
[14] A. Kejriwal, P. Bandyopadhyay, A.N. Biswas, Aromatic hydroxylation using an oxo-bridged diiron(III) complex: a bio-inspired functional model of toluene monooxygenases, Dalton Trans. 44 (2015) 17261−17267.
[15] A. Raba, M. Cokoja, W.A. Herrmann, F.E. Kühn, Catalytic hydroxylation of benzene and toluene by an iron complex bearing a chelating di-pyridyl-di-NHC ligand, Chem. Commun. 50 (2014) 11454−11457.
[16] L. Carneiro, A.R. Silva, Selective direct hydroxylation of benzene to phenol with hydrogen peroxide by iron and vanadyl based homogeneous and heterogeneous catalysts, Catal. Sci. Technol. 6 (2016) 8166−8176.
[17] G.C. Silva, N.M.F. Carvalho, A. Horn, E.R. Lachter, O.A.C. Antunes, Oxidation of aromatic compounds by hydrogen peroxide catalyzed by mononuclear iron(III) complexes, J. ;Mol. Catal. A: Chem. 426 (2017) 564−571.
[18] G. Capocasa, G. Olivo, A. Barbieri, O. Lanzalunga, S. Di Stefano, Direct hydroxylation of benzene and aromatics with H₂O₂ catalyzed by a self-assembled iron complex: evidence for a metal-based mechanism, Catal. Sci. Technol. 7 (2017) 5677−5686.
[19] O.Y. Lyakin, A.M. Zima, N.V. Tkachenko, K.P. Bryliakov, E.P. Talsi, Direct evaluation of the reactivity of nonheme iron(V)−oxo intermediates toward arenes, ACS Catal. 8 (2018) 5255−5260.
[20] N.V. Tkachenko, R.V. Ottenbacher, O.Y. Lyakin, A.M. Zima, D.G. Samsonenko, E.P. Talsi, K.P. Bryliakov, Highly efficient aromatic C-H oxidation with H₂O₂ in the presence of iron complexes of the PDP family, ChemCatChem (2018),

https://doi.org/10.1002/cctc.201800832.

[21] O.Y. Lyakin, A.M. Zima, D.G. Samsonenko, K.P. Bryliakov, E.P. Talsi, EPR spectroscopic detection of the elusive Fe^V=O intermediates in selective catalytic oxofunctionalizations of hydrocarbons mediated by biomimetic ferric complexes, ACS Catal. 5 (2015) 2702–2707.

[22] K. Suzuki, P.D. Oldenburg, L. Que Jr., Iron-catalyzed asymmetric olefin *cis*-dihydroxylation with 97% enantiomeric excess, Angew. Chem. Int. Ed. 47 (2008) 1887–1889.

[23] R.V. Ottenbacher, D.G. Samsonenko, E.P. Talsi, K.P. Bryliakov, Highly enantioselective bioinspired epoxidation of electron-deficient olefins with H$_2$O$_2$ on aminopyridine Mn catalysts, ACS Catal. 4 (2014) 1599–1606.

[24] O. Cussó, I. Garcia-Bosch, D. Font, X. Ribas, J. Lloret-Fillol, M. Costas, Highly stereoselective epoxidation with H$_2$O$_2$ catalyzed by electron-rich aminopyridine manganese catalysts, Org. Lett. 15 (2013) 6158–6161, 15.

[25] D. Shen, C. Miao, S. Wang, C. Xia, W. Sun, A mononuclear manganese complex of a tetradentate nitrogen ligand – synthesis, characterizations, and application in the asymmetric epoxidation of olefins, Eur. J. Inorg. Chem. (2014) 5777–5782.

[26] A.M. Kirillov, G.B. Shul'pin, Pyrazinecarboxylic acid and analogs: highly efficient co-catalysts in the metal-complex-catalyzed oxidation of organic compounds, Coord. Chem. Rev. 257 (2013) 732–754.

[27] J. Serrano-Plana, W.N. Oloo, L. Acosta-Rueda, K.K. Meier, B. Verdejo, E. Garsía-España, M.G. Bassallote, E. Münck, L. Que Jr., A. Company, M. Costas, Trapping a highly reactive nonheme iron intermediate that oxygenates strong C—H bonds with stereoretention, J. Am. Chem. Soc. 137 (2015) 15833–15842.

[28] K.M. Van Heuvelen, A.T. Fiedler, X. Shan, R.F. de Hont, K.K. Meier, E.L. Bominaar, E. Münck, L. Que Jr, One-electron oxidation of an oxoiron(IV) complex to form an [O=Fe^V=NR]$^+$ center, Proc. Natl. Acad. Sci. U.S.A. 109 (2012) 11933–11938.

[29] A.M. Zima, O.Y. Lyakin, K.P. Bryliakov, E.P. Talsi, On the nature of the active intermediates in iron-catalyzed oxidation of cycloalkanes with hydrogen peroxide and peracids, Mol. Catal. 455 (2018) 6–13.

[30] A.M. Zima, O.Y. Lyakin, K.P. Bryliakov, E.P. Talsi, Direct reactivity studies of non-heme iron-oxo intermediates toward alkane oxidation, Catal. Commun. 108 (2018) 77–81.

[31] O.Y. Lyakin, K.P. Bryliakov, G.J.P. Britovsek, E.P. Talsi, EPR Spectroscopic trapping of the active species of nonheme iron-catalyzed oxidation, J. Am. Chem. Soc. 131 (2009) 10798–10799.

[32] O.Y. Lyakin, K.P. Bryliakov, E.P. Talsi, EPR, ^{1}H and ^{2}H NMR, and reactivity studies of the iron—oxygen intermediates in bioinspired catalyst systems, Inorg. Chem. 50 (2011) 5526–5538.